Ionization of xenon by electrons: Partial cross sections for single, double, and triple ionization

D. Mathur and C. Badrinathan
Tata Institute of Fundamental Research, Homi Bhabha Road, Bombay 400 005, India
(Received 25 February 1985; revised manuscript received 13 May 1986)

High-sensitivity measurements of relative partial cross sections for single, double, and triple ionization of Xe by electron impact have been carried out in the energy region from threshold to 100 eV using a crossed-beam apparatus incorporating a quadrupole mass spectrometer. The weighted sum of the relative partial cross sections at 50 eV are normalized to the total ionization cross section of Rapp and Englander-Golden to yield absolute cross-section functions. Shapes of the partial cross sections for single and double ionization are difficult to account for within a single-particle picture. Comparison of the Xe^+ data with $4d$ partial photoionization cross-section measurements indicates the important role played by many-body effects in describing electron-impact ionization of high-Z atoms.

I. INTRODUCTION

Experimental data pertaining to ionization of atoms by electron impact is of great importance in the physics of high-temperature plasmas found in astrophysical objects as well as in laboratory discharges. Many plasma properties depend on the state of ionization of atoms and ions present in these plasmas. In astrophysics, ionization data form an integral part of theories of the interstellar media as well as models of stellar interiors. In terrestrial plasmas the ionization rate appears in equations describing the time evolution of the discharge in magnetic confinement fusion machines.

Although features and mechanisms of ionization of atoms by electrons have been widely explored over the last 50 years, there remain many ambiguities concerning absolute cross sections, shapes of cross-section functions, ratios of partial cross sections for single and multiple ionization, and accurate determinations of the energy dependence of ionization cross sections in the threshold region. Many of the discrepancies that exist in the literature can be attributed[1] to an inadequate appreciation on the part of experimentalists to the severity of the practical problems involved in such measurements. Consequently, even for rare-gas atoms, which would be expected to yield the most consistent results because of their inert nature and their ideal-gas character at the low pressures encountered in ionization measurements, significant discrepancies exist in the literature concerning both the shape of cross-section functions and their absolute magnitudes.

The most widely used sources of ionization cross sections for plasma modeling are scaling laws and semiempirical formulas[2] of the type due to Lotz:[3]

$$\sigma_i(E)=4.5\times10^{14}\sum_j \frac{\gamma_j}{I_jE}\ln(E/E_j)\ , \tag{1}$$

where the ionization cross section σ_i at an electron-impact energy E (in eV) is given in units of cm^2, γ_j is the number of electrons in subshell j, and I_j is the ionization energy (in eV) for electrons occupying that subshell. This formula is based on Coulomb-Born theory for infinite-Z hydrogenic ions and on experimental data for singly charged ions. A number of quantum-theoretical calculations of cross sections for electron-impact single ionization have also been carried out in Coulomb-Born[4–6] and distorted-wave[7] approximations. The unifying feature of all such descriptions of the ionization process is the fact that only direct ejection of single electrons from neutral or ionized atom is considered.

Substantial experimental evidence now exists to show that in many instances indirect mechanisms can dominate the ionization process. One such process involves excitation of a bound electron from an inner shell to a discrete bound state embedded in the ionization continuum which, upon rapid autoionization, can sometimes dominate over the direct ionization process. In the case of single ionization of Ar, structure in the ionization cross-section function for Ar^+ in the region of 45 eV has been shown[8] to be due to excitation of a $3s$ electron to ^1D and ^1P states of Ar^* which subsequently autoionize into the adjacent Ar^+ continuum. In near-threshold ionization efficiency measurements[9] in Xe^+, the use of monoenergetic electrons has revealed several sharp structures in the energy region between the $^2P_{3/2}$ and $^2P_{1/2}$ thresholds which can be attributed to excitation of $5p$ electrons to a number of Rydberg levels converging on the $^2P_{1/2}$ ionization limit and their subsequent autoionization into the $^2P_{3/2}$ continuum. Crossed-beam measurements have also shown significant enhancement[10,11] of ionization cross sections due to the excitation-autoionization process in all singly charged alkali-metal-like ions heavier than Mg^+. More recent measurements on electron-impact ionization of ions of initially higher charge[12] have shown that indirect effects become more important as ionic charge increases until the electronic states responsible for the largest indirect effects become bound, and therefore do not autoionize. In addition to the excitation-autoionization process, another indirect mechanism involves the formation of highly excited resonance states by dielectronic recombination followed by double Auger autoionization.[13,14] These recombination resonances involve inner-shell electronic excitation to

high-nl states whose dominant decay mode is double autoionization. Such resonances affect the shape of the ionization cross-section function by extending the normally expected sharp excitation onset towards lower energies.

Further difficulties are encountered when an adequate description of the ionization process in heavy atoms is sought. For instance, atoms such as xenon possess an extremely large dipole polarizability which manifests itself in very large $4d$ and $5p$ photoionization cross sections. The strongly collective nature of $4d$ electrons in Xe is indicated by the totally nonhydrogenic character of photoabsorption spectra,[15–17] as well as by the shortness of the lifetimes of radiationless transitions.[18] Consequently, theoretical models utilizing single-particle pictures of orbitals and one-electron central-field models become inadequate in describing the ionization of high-Z atoms. Comparison of experimental data with Hartree-Fock-Slater calculations[19–21] clearly illustrates the manner in which the single-particle spectrum is partly, or even totally, wiped out and that the oscillator strength is moved to higher energies. In the case of the $4d^{10}$ orbital in Xe, the single-particle strength is almost totally eliminated and reappears as a broad, structureless feature in an energy region with very low single-particle absorption. Many-body calculations of the Xe photoabsorption cross section have been more successful; the $4d$ photoionization cross section in Xe has been adequately reproduced using a plasma-type model,[22,23] the random-phase approximation with exchange. Another method[24,25] has been developed on the basis of many-body diagram expansion for atomic polarizability. Such an expansion is partially summed to infinite order to enable a nonperturbative treatment of polarization effects and to deal with collective oscillations in atomic orbitals. This method has been applied[26] to the $5p^6$ orbital in Xe to illustrate the dramatic change in the photoabsorption cross section when dynamic electron correlation is included in order to account for collective processes. Such many-body treatments lead to the conclusion that effects of dynamic electron correlations are generally too strong in high-Z atoms to be treated simply as perturbations of the Hartree-Fock atom, but have to be included in a zeroth-order approximation in much the same way as in considerations of plasma oscillations in an electron gas or collective motions in nuclei.

Experimental information on single- and multiple-ionization cross sections of Xe atoms and ions is relatively scarce. First measurements of single and multiple ionization of Xe^{q+} ($q=1$–4) have been recently reported[27,28] using a crossed-beam apparatus. These measurements reveal several unexpected features. The data obtained indicate extremely large cross sections for multiple ionizations; the ratio[29] of double to single ionization of Xe^{2+} ions for 700 eV electron-impact energy is 70%, and increases with electron energy. It is also shown that the Xe ion can become easier to ionize when its charge state is increased; the ionization cross section for Xe^{4+}-Xe^{5+} is greater than the corresponding value for Xe^{3+}-Xe^{4+} at 250 eV electron energy. In addition, unusual enhancement of ionization cross sections is observed in the 100-eV energy region; it has been postulated[27] that such effects may be a manifestation of the collective nature of electrons in certain Xe orbitals.

Although a large number of investigations have been reported for the total ionization cross section, Xe-Xe^{q+}, for all values of q, by electron impact, there remains a paucity of experimental data for partial ionization cross sections to specific charge states (see Ref. 29 for the most recent compilation of pertinent data). Partial cross sections for Xe-Xe^{q+} ($q=1$–3) have been reported in only three instances[30–32] for electron energies greater than 500 eV. There appears to be only one partial cross-section measurements reported for energies below 500 eV. We have carried out such measurements in a crossed-beam apparatus incorporating a quadrupole mass spectrometer in the electron-energy range from threshold to 150 eV. The experimental checks carried out in order to overcome the severe practical difficulties encountered in such measurements and the method by which cross-section values are deduced are described in detail in the following section.

II. EXPERIMENTAL METHOD

On the basis of their critical evaluation of different techniques used in ionization measurements, Kieffer and Dunn[1] reached the conclusion that the major problems encountered in such experiments concern (a) the collection efficiency for ions generated in the ion source of a mass spectrometer, (b) discrimination on the basis of mass-to-charge ratio, and (c) discrimination on the basis of the initial kinetic energy possessed by the ion. Ion sources of the type encountered frequently in commercial mass spectrometers used for ionization cross-section measurements usually comprise a magnetically confined electron beam and a repeller electrode which aids ion extraction by application of an appropriate electric field transverse to the electron beam. In practice, the presence of a magnetic field cannot only complicate electron- and ion-beam trajectories, but can also sometimes enhance the trapping of slow ions in an electrostatic potential well that is created within the space charge of a reasonably intense electron beam. Such trapping phenomena can lead to collisional effects which are difficult to predict quantitatively; consequently, the repeller characteristic often fails to exhibit an unambiguous saturation condition and the magnitude of the extracted flux becomes affected in an unpredictable fashion. Discrimination effects can occur at the ion source exit slit and at the mass spectrometer's entrance and exit slits, though quantitative information regarding such effects is extremely rare. Recently, a study has been made of ion-extraction characteristics as a function of electron-beam space charge and applied extraction (repeller) voltage in the widely used three-electrode Nier-type ion source,[33] and it is concluded that accurate and reliable measurement of ionization cross-section functions is not possible using such a source without extensive modifications.

The problems encountered in a conventional mass-spectrometer configuration are sought to be circumvented in the present studies by adopting a crossed electron-beam—atomic-beam geometry in conjunction with a quadrupole mass spectrometer. Only salient features pertinent to the present study are described here as the overall ap-

paratus is similar to the one described fully in our recent publications reporting threshold measurements of ionization and dissociative ionization in molecules;[34–36] a major modification has been the introduction of a faster diffusion pump (2400 $1s^{-1}$) which allows more efficient differential pumping in the collision zone and enables a base operating pressure of 2×10^{-8} Torr.

The all-important interaction region is shown in Fig. 1. A collimated electron beam of intensity 2×10^{-7} A and full width at half maximum of $\sim$120 meV intersects, at right angles, an atomic beam.

The interaction zone comprises a "surfaceless" cube, five sides of which are constructed of highly transparent (>85% transmission) molybdenum mesh with an effusive gas source in the form of a 1-mm-i.d. stainless-steel tube. Electron-impact-induced ions which drift towards the sixth side of the cube (in the direction of the atomic beam) are extracted by a weak three-element lens into a quadrupole mass spectrometer capable of giving unit mass resolution up to mass 300. All electrodes in the immediate vicinity of the interaction zone are kept at the same potential as the molybdenum mesh (Fig. 1). We have no repeller voltage; ions are extracted by means of a penetrating field in the extraction region. Computer-calculated ion trajectories[37] have shown that in such a case all ions starting within a given region are extracted through the orifice. In our case, the acceptance solid angle of the ion optical system preceding the quadrupole mass filter is $\pi/12$ rad, which ensures that the overlap volume between the electron and atomic beams (solid angle equal to $\pi/32$ rad) is well within the field of view over the entire range of electron energies. We have measured the variation of Xe^+ and Xe^{2+} ion flux transmitted through the quadrupole filter as a function of the kinetic energy imparted to these ions by the extraction voltage. Typical data for two different electron-impact energies are shown in Fig. 2. In all cases we observe that at the lowest values of extraction voltage there is a region of constant ion flux. As the transmission efficiency of a quadrupole mass filter is inversely proportional to the square of quadrupole field,[37] at higher values of extraction voltage the ion flux detected increases; unambiguous saturation conditions are seldom reached. All measurements reported here were taken with an ion energy of 0.5 eV, where the ion transmission efficiency is not only observed to be constant up to an ion energy of about 3 eV, but is also independent of electron-impact energy up to 160 eV in the case of Xe^+ and up to 100 eV in the case of Xe^{2+} and Xe^{3+}.

One implication of the low kinetic energy possessed by the ions is that the relatively long time such ions spend in the fringing field that inevitably exists near the entry plane of the quadrupole filter can result in defocusing action and consequent loss in transmission. In order to minimize the effect of the fringing fields we have inserted an earthed plate (EO in Fig. 1) with a small axial orifice which provides an additional advantage in that loss of ion flux due to axial dispersion is also minimized.

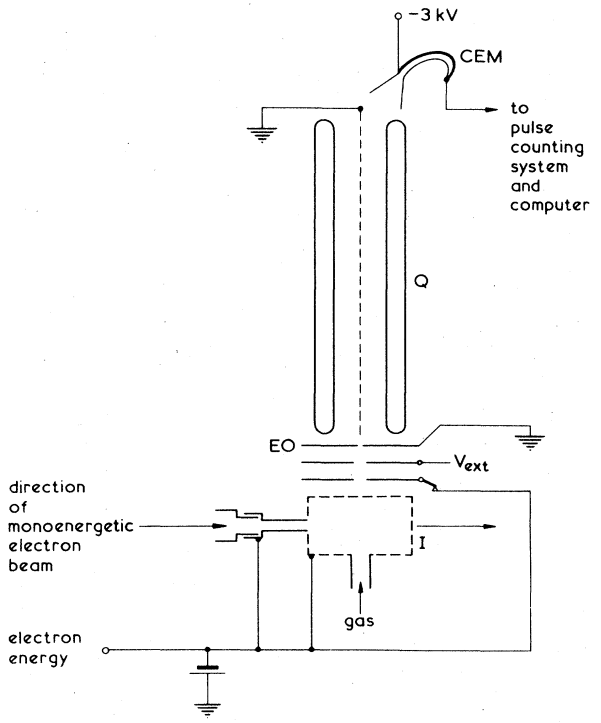

FIG. 1. Schematic diagram of the interaction zone. *I*, high-transparency molybdenum mesh; V_{ext}, extraction voltage which produces a penetrating field into the collision region; EO, entrance orifice into the mass analyzer; *Q*, quadrupole mass filter rods; CEM, off-axis channel electron multiplier operating in the particle-counting mode.

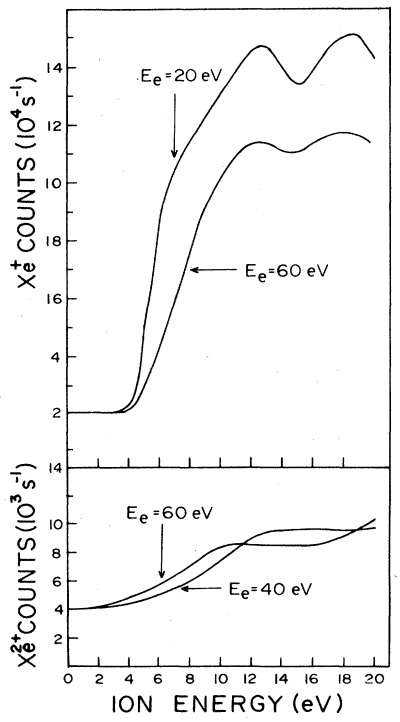

FIG. 2. Variation of singly charged and doubly charged ion flux as a function of ion energy imparted by the penetrating extraction field at different electron energies.

We have also attempted to ensure that the transmission efficiency of our mass filter is not dependent upon the charge-to-mass ratio of the ions. Such a condition of nearly zero-mass discrimination is difficult to achieve because, as pointed out above, the heavier the ion the longer the time it spends in the fringing fields and, consequently, the larger the dispersion it experiences in the quadrupole field. As a result, there is always a tendency for the heavier ions to be transmitted less efficiently, thus resulting in mass discrimination, particularly at high resolutions. The variation of a quadrupole filter's sensitivity as a function of mass resolution has been measured[38] for Xe^+ and Xe^{2+} ions, for an ion source geometry which is similar to the one used in the present measurements. Results indicate that at resolving powers up to about 150, the sensitivity curves for both singly and doubly charged species are coincident, indicating negligible mass discrimination. As the resolving power is increased the curves diverge, the lower mass (Xe^{2+}) having the higher sensitivity. In the present measurements the instrumental resolving power was kept fixed at a value of 130, and extreme care was exercised to ensure that the crossed-beam geometry corresponded closely to that described in Ref. 38. Both the electron-beam and atomic-beam cross-sectional areas were 1 mm^2 each and the overlap volume was always along the axis of the quadrupole rods; any deviation from the chosen interaction volume (due to misalignment, etc.) would generally result in almost zero overlap and, consequently, an indication was available in the form of a very small ion signal.

It is known that radial as well as axial trapping of slow ions[39] can occur in the space charge of any reasonably intense cylindrical electron beam. Confinement of ions within such electron beams enabled Baker and Hasted[40] to perform early measurements of electron-ion cross sections. The importance of confinement was realized as a result of the appearance of doubly charged rare-gas ions just above the potential corresponding to the difference between the first and second ionization potentials, in abundance proportional to the square of the electron-beam intensity. We have measured the variation of ion current with electron-beam current for all the ion charges reported here; a typical curve for Xe^{2+}, shown in Fig. 3, indicates a departure from linearity for electron currents larger than about 0.35 μA. Our measurements indicate that the overall shape of the ionization efficiency function for all the ions changes markedly as a function of electron-beam current. In order to be free from stray fields and confinement effects due to the space charge within the electron beam, all measurements reported here were conducted with electron-beam currents less than 0.05 μA, in a region where a linear relationship could be demonstrated between ion signal and the electron-beam intensity.

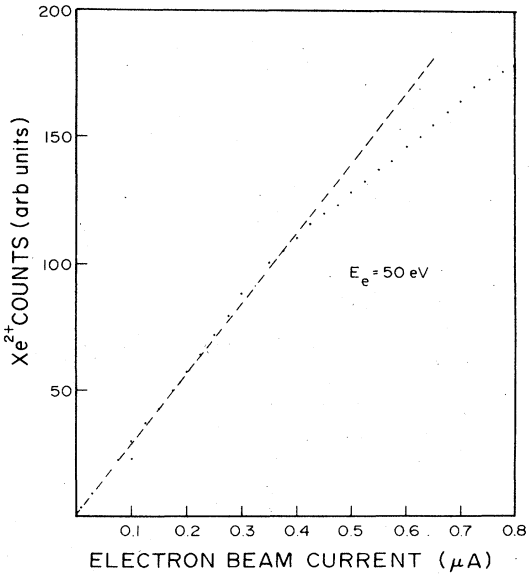

FIG. 3. Variation of Xe^{2+} flux with electron-beam current. Normal operating electron current was always kept below 0.05 μA.

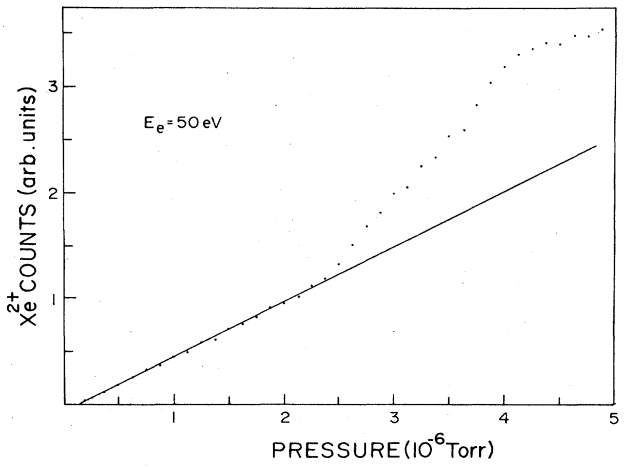

FIG. 4. Variation of Xe^{2+} flux with gas pressure.

A typical curve showing the dependence of Xe^{2+} flux on Xe gas pressure is shown in Fig. 4. Our operating pressure was always in the region of 5×10^{-8} Torr, well within "single-collision conditions."

Ion detection in the present measurements was by means of a channel electron multiplier operating in the particle-counting mode. The detector was mounted off axis in order to eliminate the possibility of counting energetic neutral particles or photons. The detection efficiency of such a multiplier has been measured as a function of ion energy for a large range of ion masses[41] and found to be constant for the energy range 2.5—12 keV. In the present case the front cone of the multiplier was operated at -3 kV; the kinetic energies of Xe^+, Xe^{2+}, and Xe^{3+} ions impinging on the entrance cone were all within the range of energy where the detection efficiency is constant. Thus, a measurement of the ratio of doubly charged ion flux to singly charged flux pertains to a ratio of the two ionization cross sections at a given electron energy.

III. RESULTS AND DISCUSSION

Following the experimental method outlined in the preceding section, relative partial ionization cross section

functions have been measured for the following processes:

$$e + \mathrm{Xe} \rightarrow \mathrm{Xe}^{+} + 2e$$
$$\rightarrow \mathrm{Xe}^{2+} + 3e$$
$$\rightarrow \mathrm{Xe}^{3+} + 4e \ .$$

The electron-energy scale in each case has been calibrated with reference to the $^2P_{3/2}$ onset for Xe^+ production at 12.13 eV, using the vanishing-current method.[35,36] This calibration is believed to be accurate to within ± 0.08 eV. We have also determined cross-section ratios $\sigma_i(Xe^{2+})/\sigma_i(Xe^+)$ and $\sigma_i(Xe^{3+})/\sigma_i(Xe^+)$ at 100 eV electron-impact energy. Using these measured ratios it is possible to calibrate the relative partial ionization cross-section functions for double and triple ionization with that for single ionization; the charge-weighted sum of these calibrated cross sections yields the relative total ionization cross-section function, which can then be normalized to the well-established absolute total ionization cross-section data of Rapp and Englander-Golden.[42] In the present measurements, the ratio of double to single ionization was determined to be 0.116 at 100 eV electron energy, whereas the ratio for triple to single ionization was 0.022 at the same electron energy. In measuring these ratios, the sum of the ion counts under all the Xe isotope peaks in a mass spectrum was considered. On the basis of data accumulated over a period of several months, the maximum statistical deviations for the measured ratios are of the order of $\pm 3\%$ for $\sigma_i(Xe^{2+})/\sigma_i(Xe^+)$ and $\pm 5\%$ for $\sigma_i(Xe^{3+})/\sigma_i(Xe^+)$. Comparison of our measured ratios with other data is difficult because transmission problems inherent in the previously used commercial ion spectrometers make it difficult to measure correct relative abundances of the different charge states of ions produced by electron impact. This is reflected in the discrepancies existing between the results of the relatively few measurements that have been reported for Xe. At energies below 250 eV, only four other sets of cross-section ratios have been reported, and these are compared with the present data in Table I. The relatively recent measurements of Egger and Mark[43] yield lower ratios than the earlier measurements of Tate and Smith[44] and Fox;[45] the most recent data, by Stephan and Mark,[46] are in good accord with our ratio determinations.

The total ionization cross section deduced on the basis of the measured ratios is normalized to the absolute data of Rapp and Englander-Golden at an electron energy of 50 and 100 eV. A comparison of the two total cross-section functions is shown in Fig. 5. The measurements of Rapp and Englander-Golden were conducted in an ionization tube without mass analysis, with great care taken to ensure complete collection of both electron as well as ion currents; the relative accuracy of this absolute data is claimed to be better than $\pm 1\%$. The agreement between the two data functions shown in Fig. 5 is good, particularly in the low-energy region, in the case where normalization is done at 50 eV electron-impact energy. The maximum deviation between the two ionization cross sections

TABLE I. Partial ionization cross-section ratios for production of multiply to singly charged xenon ions by 100 eV electron impact on neutral Xe.

$\sigma_i(Xe^{2+})/\sigma_i(Xe^+)$	$\sigma_i(Xe^{3+})/\sigma_i(Xe^+)$	References
0.17	0.026	44
0.28	0.050	45
0.15	0.025	43
0.11	0.015	46
0.116	0.022	Present data

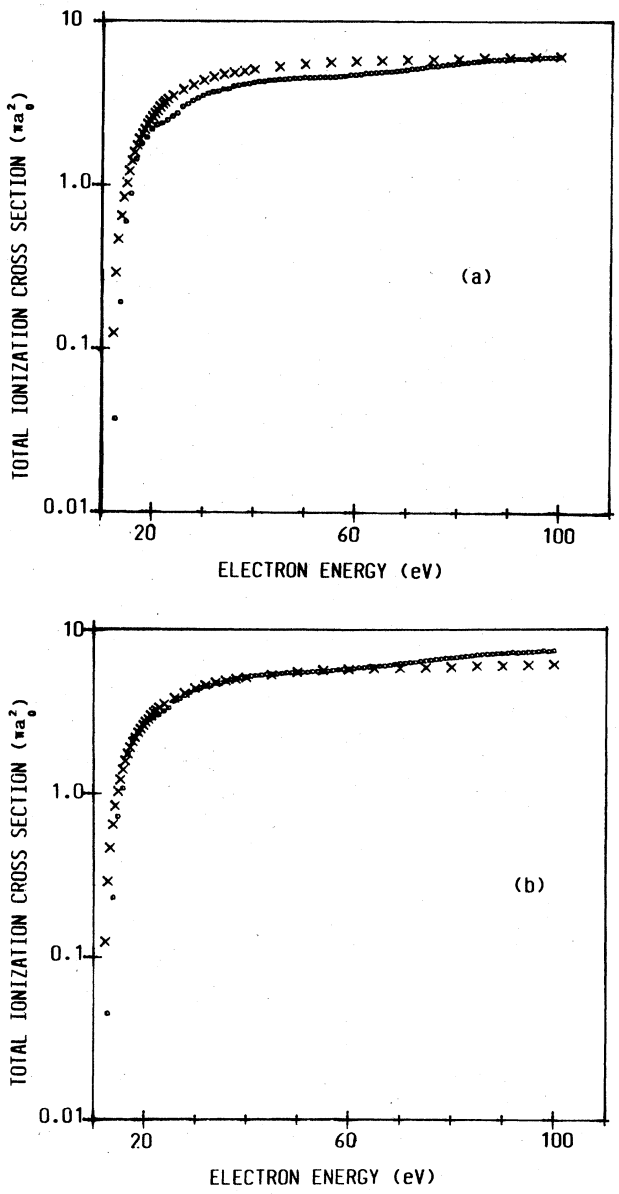

FIG. 5. Total ionization cross-section function for electron-impact ionization of Xe obtained by normalizing weighted sum of relative partial ionization cross sections to the absolute data of Rapp and Englander-Golden (Ref. 42) at (a) 100 eV electron energy and (b) 50 eV electron energy [open circles, present data; crosses, data from Rapp and Englander-Golden (Ref. 42)].

occurs in the threshold region; this is to be expected because of differences in the electron energy distribution in the two measurements. In the case where normalization is done at 100 eV the deviation between the two data sets is more marked. This comparison of total ionization cross-section functions allows an absolute normalization of the relative partial ionization cross-section functions using the normalization of our relative data to absolute data at an energy of 50 eV [Fig. 5(b)]. Such an absolute partial cross-section function for single ionization of neutral Xe is shown in Fig. 6. In an earlier report we had presented the single ionization cross section data for Xe in which normalization of our relative measurements to the absolute data of Rapp and Englander-Golden was carried out at an electron energy of 20 eV, below the threshold for double or triple ionization.[47] However, the present method is believed to yield much more reliable cross section values.

The shape of the Xe^+ function observed in our measurements is similar to that obtained by Stephan and Mark.[46] These authors did not seek to explain the observed shape but, instead, compared their measured cross section magnitude with calculated cross section functions using various classical and semiclassical binary encounter models. In the light of the discussion which follows it will be obvious that any attempt to explain the ionization process in Xe in terms of such theories will not be totally successful.

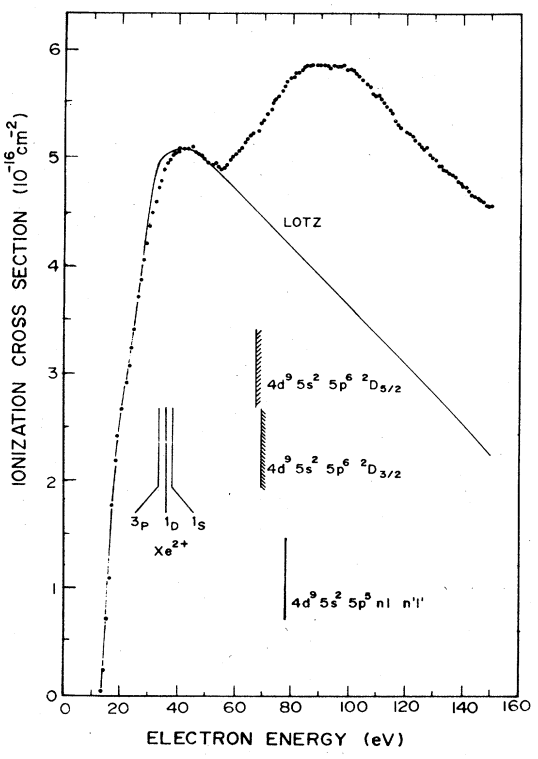

FIG. 6. Cross section for single ionization of Xe by electron impact. Solid line is the Lotz formula fitted to experimental data between threshold and 50 eV (see text).

The partial cross-section function for single-electron ejection from xenon (Fig. 6) shows a peak at 40 eV (which corresponds to 3.3 times the threshold energy), a minimum in the region of 52 eV, followed by a broad maximum centered at 95 eV. The structure observed is somewhat similar to that observed in the Ar^+ ionization cross-section function at an energy of 45 eV, which was interpreted[8,48] as being due to excitation of a $3s$ electron to ^1D and ^1P states of highly excited neutral Ar, which subsequently autoionize into the adjacent Ar^+ continuum. If a similar excitation-autoionization explanation is sought in the case of Xe^+, electronic states which can be considered as likely candidates are those involving excitation of electrons from the $4d$ orbital to Rydberg series which converge on the $^2D_{5/2,3/2}$ ionization limits. From electric dipole selection rules it is most probable that the series leading to these limits will be due to excitation to a p or f outer subshell. The earliest photoabsorption experiments using synchrotron radiation[49] produced evidence that excitation of $4d$ electrons is predominantly to a p level, corresponding to the transition

$$4d^{10}5s^25p^6,{}^1S_0 - 4d^95s^25p^6({}^2D_{3/2,5/2})np,{}^1P_1 .$$

Prominent lines in the optical spectrum were correlated with transitions to a series of np levels ($6 \leq n \leq 10$) starting at 65.11 eV and converging to the $^2D_{5/2}$ limit at 67.55 eV, and another similar series starting at 67.04 eV which converged on the $^2D_{3/2}$ limit at 69.52 eV. Taking these energies into account it appears most unlikely that the excitation-autoionization process involving these levels could account for the dip observed in the single-ionization cross-section function at a much lower energy (52 eV).

Doubly excited autoionizing electronic states having configurations $5s^15p^5nln'l'$ or $4d^95p^5nln'l'$ are also unlikely candidates for explaining the structure observed in Fig. 6, as the former lie at energies well below 48 eV, whereas the latter occur in the region of 75 eV. Removal of two outermost $5p$ electrons results in a Xe^{2+} ion in the ^3P ground state (33.33 eV) and two low-lying excited states, ^1D (35.4 eV) and ^1S (37.96 eV). Thresholds for the opening of these channels also occur at energies far removed from the region where the Xe^+ structure is observed.

It is clear that indirect processes such as excitation-autoionization cannot be invoked to explain the structure observed in Fig. 6. In order to postulate some other mechanism, we have to consider the special properties of electrons in the $4d$ orbital in Xe.

It is now established that the totally nonhydrogenic character of $4d$-ϵf photoabsorption spectra in Xe may be considered as the first clear indication of the importance of collective effects in high-Z atoms. The "delayed-onset" effect was first observed by Lukirshii *et al.*[15] and, independently, by Ederer,[16] and was first explained by Cooper.[19] The term "delayed onset" pertains to the usual situation in an optical spectrum where the signal due to photoionization is normally large in the immediate vicinity of threshold, and then decreases monotonically as the energy increases. In the $4d$ photoabsorption spectra in Xe, however, the oscillator strength for a $4d$-ϵf transition was extremely small at threshold; it then increased rapidly

(by a factor of 15) to a prominent maximum at an energy 20 eV above threshold. Cooper[19] showed that such a result could be understood qualitatively in terms of the variation of the electric dipole matrix element with energy. It was suggested that the suppression of d-f transitions near threshold was due to a centrifugal repulsion potential superimposed on the attractive Coulomb potential which gave rise to a potential barrier in which continuum states of high angular momentum are held out from the center when the kinetic energy of the ejected electron is low. As the kinetic energy increases, so does the penetration into the barrier. Hence, the spatial overlap between the initial and final states is an increasing function of energy until, eventually, the negative part of the wave function begins to overlap with the $4d$ wave function and phase cancellation leads to a gradually decreasing cross section. Although the potential barrier concept provided a useful qualitative guide to interpreting the $4d$-ϵf photoabsorption spectrum, electron-electron correlations were still not accounted for. Such correlations must be expected to be important in the threshold region where the ejected electron has barely enough kinetic energy to escape from the atom; its motion cannot therefore be adequately described by a local central field. Such considerations provided the stimulus for the application of many-body theory by Amusia and co-workers[22,23] and Wendin.[24–26]

In order to probe the difference between the shape of our Xe^+ data (Fig. 6) and that predicted on the basis of a single-electron "knock-out" picture of ionization, we have fitted the semiempirical Lotz[3] formula to our data between the threshold region and 50 eV, taking account of direct ejection of a single electron from the $5p$ and $5s$ orbitals. The difference between the fitted cross section and our data is shown in Fig. 7 as a broad, asymmetrical peak centered at 95 eV. It is of interest to note that the Lotz cross section for direct ejection of a single electron from the $4d$ orbital yields a totally different shape, whereas the

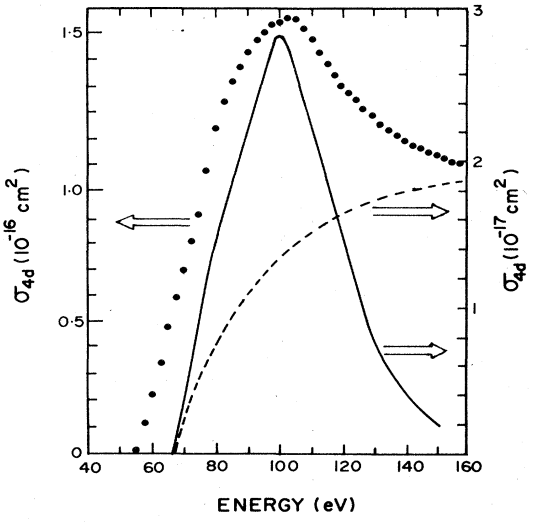

FIG. 7. Cross section for ionization of a $4d$ electron in Xe. Dots, present data; solid line, photoabsorption measurements (Ref. 50); dashed line, calculated using Lotz formula (Ref. 3).

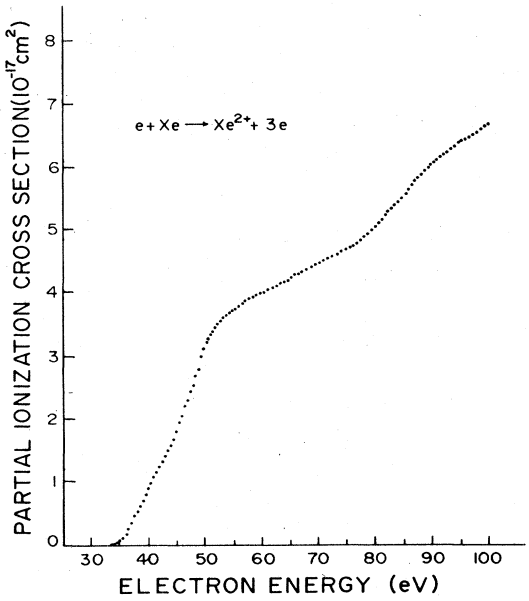

FIG. 8. Partial cross section for double ionization of Xe.

present data are surprisingly similar in shape to the $4d$ partial photoionization cross-section function,[50] as well as to the $4d$ spectrum calculated by Amusia *et al.*[22] using a plasma-type model, the random-phase approximation with exchange.

Partial cross-section functions for double and triple ionization of neutral Xe are shown in Figs. 8 and 9. Since double-electron ejection results in two outgoing Coulomb waves, the onset for Xe^{2+} production is observed to be more gradual in the threshold region when compared with

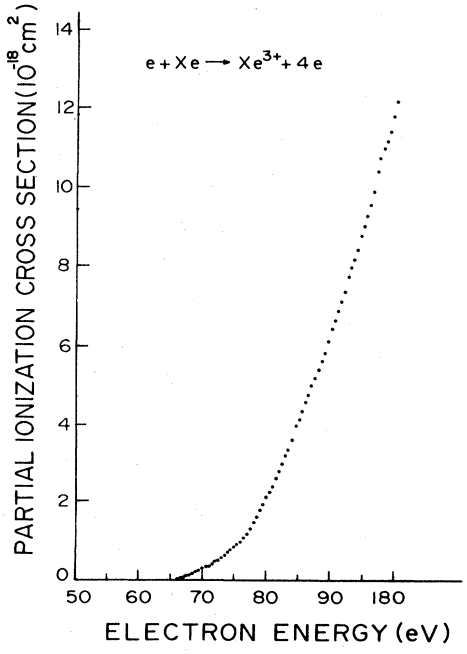

FIG. 9. Partial cross section for triple ionization of Xe.

TABLE II. Absolute partial cross section for single ionization of Xe.

Energy (eV)	σ_i (10^{-16} cm^2)	Energy (eV)	σ_i (10^{-16} cm^2)	Energy (eV)	σ_i (10^{-16} cm^2)
13	0.046	63	5.094	113	5.433
14	0.231	64	5.13	114	5.397
15	0.738	65	5.167	115	5.372
16	1.101	66	5.179	116	5.324
17	1.767	67	5.179	117	5.3
18	2.19	68	5.215	118	5.264
19	2.396	69	5.276	119	5.239
20	2.674	70	5.312	120	5.215
21	2.856	71	5.348	121	5.179
22	2.916	72	5.409	122	5.167
23	3.049	73	5.457	123	5.13
24	3.231	74	5.518	124	5.094
25	3.376	75	5.542	125	5.07
26	3.678	76	5.578	126	5.046
27	3.836	77	5.627	127	5.058
28	4.017	78	5.663	128	4.985
29	4.175	79	5.687	129	4.961
30	4.332	80	5.699	130	4.937
31	4.453	81	5.748	131	4.901
32	4.562	82	5.76	132	4.888
33	4.683	83	5.772	133	4.84
34	4.755	84	5.808	134	4.828
35	4.804	85	5.82	135	4.828
36	4.864	86	5.808	136	4.816
37	4.901	87	5.82	137	4.792
38	4.937	88	5.82	138	4.755
39	4.985	89	5.82	139	4.731
40	5.009	90	5.82	140	4.707
41	5.034	91	5.82	141	4.695
42	5.034	92	5.82	142	4.659
43	5.034	93	5.772	143	4.659
44	5.046	94	5.808	144	4.634
45	5.058	95	5.808	145	4.61
46	5.009	96	5.808	146	4.598
47	4.997	97	5.808	147	4.574
48	4.973	98	5.808	148	4.562
49	4.937	99	5.76	149	4.525
50	4.913	100	5.772	150	4.525
51	4.900	101	5.772	151	4.513
52	4.888	102	5.723	152	4.489
53	4.901	103	5.711	153	4.465
54	4.876	104	5.675	154	4.465
55	4.852	105	5.711	155	4.465
56	4.864	106	5.639	156	4.441
57	4.901	107	5.614	157	4.429
58	4.937	108	5.554	158	4.417
59	4.973	109	5.542	159	4.429
60	4.997	110	5.53	160	4.404
61	5.022	111	5.506	161	4.404
62	5.07	112	5.469	162	4.38

sharp Xe^+ onset. The vanishing-current method yields an onset energy of 33.40 ± 0.08 eV, which compares favorably with the spectroscopically defined energy of 33.327 eV for the ^3P ground state of Xe^{2+}. We do not observe any contribution from excitation-autoionization processes involving Rydberg series converging on the ^1D (35.4 eV) and ^1S (37.96 eV) excited states. Removal of an electron each from the $5s$ and $5p$ orbitals to yield $^3P_{2,1,0}$ and ^1P states, respectively, becomes energetically possible at 45.5 eV; the onset for removal of both $5s$ electrons is in the region of 60 eV. None of these processes appears to have a significant effect on the Xe^{2+} partial ionization cross-

TABLE III. Absolute partial cross section for double ionization of Xe.

Energy (eV)	σ_i (10^{-16} cm^2)	Energy (eV)	σ_i (10^{-16} cm^2)	Energy (eV)	σ_i (10^{-16} cm^2)
35	0.013	58	0.385	81	0.512
36	0.028	59	0.389	82	0.522
37	0.045	60	0.393	83	0.532
38	0.062	61	0.397	84	0.538
39	0.079	62	0.403	85	0.551
40	0.099	63	0.424	86	0.565
41	0.116	64	0.41	87	0.577
42	0.132	65	0.414	88	0.587
43	0.149	66	0.422	89	0.592
44	0.168	67	0.426	90	0.6
45	0.192	68	0.431	91	0.609
46	0.219	69	0.434	92	0.616
47	0.24	70	0.438	93	0.621
48	0.267	71	0.443	94	0.629
49	0.297	72	0.446	95	0.634
50	0.318	73	0.451	96	0.641
51	0.336	74	0.455	97	0.647
52	0.348	75	0.46	98	0.651
53	0.351	76	0.471	99	0.646
54	0.37	77	0.476	100	0.66
55	0.365	78	0.483		
56	0.372	79	0.492		
57	0.378	80	0.501		

section function. The structure seen in Fig. 8 in the region of 55 eV is similar to that observed in double-photoionization measurements.[51] The partial cross section for triple ionization (Fig. 9) shows a featureless curve whose threshold is measured to be 66.15 ± 0.10 eV. Cairns *et al.*[51] have used one-electron wave functions[52] to compute the probabilities for double and triple photoionization in the energy region above 55 eV; they concluded that photoionization of many-electron atoms could not be described adequately by the usual one-electron central-field model.

TABLE IV. Absolute partial cross section for triple ionization of Xe.

Energy (eV)	σ_i (10^{-16} cm^2)	Energy (eV)	σ_i (10^{-16} cm^2)
66	0.000 73	84	0.038
67	0.0015	85	0.043
68	0.0021	86	0.047
69	0.0029	87	0.052
70	0.0041	88	0.056
71	0.0044	89	0.06
72	0.0059	90	0.066
73	0.0069	91	0.071
74	0.099	92	0.076
75	0.01	93	0.083
76	0.011	94	0.087
77	0.014	95	0.093
78	0.017	96	0.099
79	0.019	97	0.108
80	0.022	98	0.114
81	0.025	99	0.118
82	0.029	100	0.126
83	0.033		

Other experimental evidence which highlights the importance of an indirect ionization process comes from the field of electron-ion collisions. Measurement of the single-ionization cross section for Xe^{3+} ions by Gregory *et al.*[53] revealed a prominent maximum in the vicinity of 100 eV. Later measurements of double ionization of Xe^{q+} ($q = 1$–4) ions by Ahchenbach *et al.*[54] demonstrated the importance of a two-step process involving single ionization of electrons in the $4d$ orbital and subsequent autoionization. Additionally, the cross section $\sigma^{4d}_{q,q+2}$ assigned to this indirect process was found to nearly coincide with the partial $4d$ photoionization cross section.

IV. SUMMARY AND CONCLUSIONS

High-sensitivity measurements of partial cross-section functions for single, double, and triple ionization of neutral Xe by electrons have been carried out in a crossed-beam apparatus incorporating a quadrupole mass spectrometer. Accurate values of the ratio for double to single and triple to single ionization have been determined at 100 eV energy. We normalize the weighted sum of the relative partial cross sections determined at this electron energy to the value of the total ionization cross section reported by Rapp and Englander-Golden and deduce partial cross sections for single, double and triple ionization of Xe (see Tables II–IV). In view of the many uncertainties inherent in our measurement technique as well as in our normalization procedure we estimate that the overall accuracy of our cross section values cannot be better than $\pm 20\%$.

The energy dependence of the partial cross sections for Xe^+ and Xe^{2+} production has structure which is totally different from that which can be expected on the basis of simple models which do not include the many-body character of the electronic interactions involved. Indirect processes involving the excitation-autoionization mechanism do not account for the observed structure.

In common with the conclusions reached in recent electron-ion experiments, our data also indicate that the ionization process in complex atoms cannot be adequately described within the one-electron, central-field framework. It appears reasonable to postulate that collective effects and concepts such as electron-electron correlations and collapse of wave functions, which have been extensively discussed in the context of photoionization, must be considered for electron-impact ionization of high-Z atoms too.

ACKNOWLEDGMENTS

We are grateful to Professor E. Salzborn for sending us copies of his work prior to publication. We also thank Professor S. K. Bhattacherjee and Professor S. K. Mitra for allowing us laboratory facilities to pursue these studies and Dr. S. V. Krishna Kumar for illuminating discussions.

[1]L. J. Kieffer and G. H. Dunn, Rev. Mod. Phys. **38**, 1 (1966).
[2]D. E. Post, R. V. Jensen, C. B. Tarter, W. H. Grasberger, and W. A. Lokhe, At. Data Nucl. Data Tables **20**, 397 (1977).
[3]W. Lotz, Z. Phys. **216**, 241 (1968).
[4]L. B. Golden and D. H. Sampson, J. Phys. B **20**, 2229 (1977); **11**, 3235 (1978); **13**, 2645 (1980).
[5]D. L. Moores, J. Phys. B **11**, L403 (1978).
[6]M. R. H. Rudge and S. B. Schwartz, Proc. Phys. Soc. London **88**, 563 (1966).
[7]S. M. Younger, Phys. Rev. A **25**, 3396 (1982); **26**, 3177 (1982), and references therein.
[8]D. Mathur and C. Badrinathan, Int. J. Mass Spectrom. Ion Proc. **52**, 167 (1984).
[9]D. Mathur and D. C. Frost, J. Chem. Phys. **75**, 5381 (1981).
[10]S. O. Martin, B. Peart, and K. T. Dolder, J. Phys. B **1**, 537 (1968).
[11]B. Peart and K. T. Dolder, J. Phys. B **1**, 872 (1968).
[12]D. C. Gregory, P. F. Dittner, and D. H. Crandall, Phys. Rev. A **27**, 724 (1983), and references therein.
[13]K. J. La Gattuta and Y. Hahn, Phys. Rev. A **24**, 2273 (1981).
[14]R. W. Henry and A. Msezane, Phys. Rev. A **26**, 2545 (1982).
[15]A. P. Lukirshii, I. A. Brytov, and T. M. Zinkina, Opt. Spektrosk. **17**, 405 (1964) [Opt. Spectrosc. **17**, 234 (1964)].
[16]D. L. Ederer, Phys. Rev. Lett. **13**, 760 (1964).
[17]R. Haensel, G. Keitel, and P. Schreiber, Phys. Rev. **188**, 1375 (1969).
[18]U. Fano and J. W. Cooper, Rev. Mod. Phys. **40**, 441 (1968).
[19]J. W. Cooper, Phys. Rev. Lett. **13**, 762 (1964).
[20]S. T. Manson and J. W. Cooper, Phys. Rev. **165**, 126 (1968).
[21]E. J. McGuire, Phys. Rev. **175**, 20 (1968).
[22]M.Ya. Amusia, N. A. Cherepkov, and L. V. Chernysheva, Zh. Eksp. Teor. Fiz. **60**, 160 (1971) [Sov. Phys.—JETP **33**, 90 (1971)].
[23]M.Ya. Amusia and N. A. Cherepkov, Case Studies At. Phys. **5**, 47 (1975).
[24]G. Wendin, in *Les Houches, Session XXXVIII, 1982—New Trends in Atomic Physics,* edited by G. Grynberg and R. Stora (North-Holland, Amsterdam, 1984), p. 555.
[25]G. Wendin and M. Ohno, Phys. Ser. **14**, 148 (1976).
[26]G. Wendin, Phys. Lett. **37A**, 445 (1971).
[27]C. Ahchenbach, A. Muller, E. Salzborn, and R. Becker, J. Phys. B **17**, 1405 (1984); Phys. Rev. Lett. **50**, 2070 (1983).
[28]A. Muller, C. Ahchenbach, E. Salzborn, and R. Becker, J. Phys. B **17**, 1427 (1984).
[29]H. Tawara, T. Kato, and M. Ohnishi, Report No. IPPI-AM-37, Institute of Plasma Physics, Nagoya University, Nagoya 464, Japan, 1985 (unpublished).
[30]B. L. Schram, Physica **32**, 197 (1966).
[31]P. Nagy, A. Shutlartz, and V. Schmidt, J. Phys. B **13**, 1249 (1980).
[32]Th.M. El-Sherbini, M. J. Van der Wiel, and F. J. deHeer, Physica **48**, 157 (1970).
[33]T. D. Mark and A. W. Castleman, Jr., J. Phys. B **13**, 1121 (1980); T. D. Mark, in *Electron-Molecule Interactions and Their Applications,* edited by L. G. Christophorou (Academic, New York, 1984).
[34]D. Mathur, J. Phys. B **13**, 4703 (1980).
[35]A. Maccoll and D. Mathur, Org. Mass Spectrom. **16**, 281 (1981).
[36]D. Mathur, Int. J. Mass Spectrom. Ion Phys. **40**, 235 (1981).
[37]W. Paul, H. P. Reinhard, and U. von Zahn, Z. Phys. **152**, 143 (1958).
[38]W. E. Austin, A. E. Holme, and J. H. Leck, in *Quadrupole Mass Spectrometry and its Applications,* edited by P. H. Dawson (Elsevier, Amsterdam, 1976), p. 143.
[39]J. B. Hasted, in *Physics of Ion-Ion and Electron-Ion Collisions,* edited by F. Brouillard and J. W. McGowan (Plenum, New York, 1983), p. 461.
[40]F. A. Baker and J. B. Hasted, Philos. Trans. R. Soc. London, Ser. A **261**, 3 (1966).
[41]C. N. Burrows, A. J. Lieber, and V. T. Zaviantseff, Rev. Sci. Instrum. **38**, 1477 (1967).
[42]D. Rapp and P. Englander-Golden, J. Chem. Phys. **43**, 1464 (1965).
[43]F. Egger and T. D. Mark, Z. Naturforsch. Teil A **33**, 1111 (1978).
[44]J. T. Tate and P. T. Smith, Phys. Rev. **46**, 773 (1934).
[45]R. E. Fox, J. Chem. Phys. **33**, 200 (1960).
[46]K. Stephan and T. D. Mark, in *Electronic and Atomic Collisions,* edited by S. Datz (North-Holland, Amsterdam, 1982), p. 265.
[47]D. Mathur and C. Badrinathan, Int. J. Mass Spectrom. Ion Proc. **68**, 9 (1986).
[48]A. Crowe, J. A. Preson and J. W. McConkey, J. Chem. Phys. **57**, 1620 (1972)
[49]K. Codling and R. P. Madden, Phys. Rev. Lett. **12**, 106 (1964).
[50]R. Haensel, G. Keitel, P. Schreiber, and C. Kunz, Phys. Rev. **188**, 1375 (1969).
[51]R. B. Cairns, H. Harrison, and R. I. Schoen, Phys. Rev. **183**, 52 (1969).
[52]F. Hermann and S. Skillman, *Atomic Structure Calculations* (Prentice-Hall, New York, 1963).
[53]D. C. Gregory, P. F. Dittner, and D. H. Crandall, Phys. Rev. A **27**, 724 (1983).
[54]C. Ahchenbach, A. Muller, E. Salzborn, and R. Becker, J. Phys. B **17**, 1405 (1984).